Drag, ablation and fragmentation of a meteor body in the atmosphere

Vladimir Vinnikov Maria Gritsevich Daria Kuznetsova
Vladislav Lukashenko
morven9@yandex.ru

Abstract

Meteorite studies represent a low-cost opportunity for probing the cosmic matter that reaches the Earth's surface and thus for revealing the nature and origin of our Solar system. Therefore correct interpretation of fireball observations is a highly important task, since it could promptly confirm fresh meteorite fall, and furthermore provide a link to its parent body. Based on the analysis of the fireball aerodynamic equations we describe the possible results that might accompany collisions of cosmic bodies with the Earth's atmosphere and surface. After integrating, these equations well characterize the body's trajectory in the atmosphere, while the exact derived dependency of body's velocity on the height of the fireball can be further compared to the observations. The solution depends on three key dimensionless parameters defining the meteoroid drag, mass loss and rotation rate in the atmosphere. These parameters are evaluated for a number of bright meteors observed by the Canadian, Prairie and European Fireball Networks.

Introduction

The physical problem of the meteor body deceleration in the atmosphere has been considered in the number of papers and monographs, see e.g. [1]. The classical dynamic third-order system has been constructed, where the body mass $M(t)$, its height above the planetary surface $h(t)$ and its velocity $V(t)$ are the phase variables. The equations of motion projected onto the tangent and to the normal to the trajectory appear as

$$M\frac{dV}{dt} = -D + P\sin\gamma, \tag{1}$$

$$MV\frac{d\gamma}{dt} = P\cos\gamma - \frac{MV^2}{R}\cos\gamma - L, \tag{2}$$

$$\frac{dh}{dt} = -V\sin\gamma, \tag{3}$$

where $D = 1/2c_d\rho_a V^2 S$ is the drag force, $L = 1/2c_L\rho_a V^2 S$ is the lifting force, and $P = Mg$ is the body weight. Here M and V are the body mass and velocity, respectively; t is the time; h is the height above the planetary surface; γ is the local angle between the trajectory and the horizon, S is the area of the middle section of the body; ρ_a is the atmospheric density; g is the acceleration due to gravity; R is the planetary radius; c_d and c_L are the drag coefficient and the lift coefficient, respectively.

Eqs. (1)-(3) are complemented by the equation for the variable mass of the body:

$$H^*\frac{dM}{dt} = -\frac{1}{2}c_h\rho_a V^3 S\,, \tag{4}$$

where H^* is the effective enthalpy of destruction and c_h is the coefficient of heat exchange. It is assumed that the entire heat flux from the ambient gas is spent to the evaporation of the surface body material. Using Eq. (3), we will take h as a new variable in the equations and pass to the convenient dimensionless quantities

$$M = M_e m,\ V = V_e v,\ h = h_0 y,\ \rho_a = \rho_0 \rho,\ S = S_e s,$$

where h_0 is the height of the homogeneous atmosphere, ρ_0 is the atmospheric density near the planetary surface, and the subscript e indicates the parameters at the entry to the atmosphere. Since the velocities in the problem under consideration are high enough (in the range from 11 to 72 km/s), the object weight P in Eq. (1) is conventionally neglected. Variations in a slope γ are not significant and usually they are not taken into account. With allowance for the above considerations, the equations for calculating the trajectory derived from Eqs. (1), (3) and (4) eventually acquire the following simple form:

$$m\frac{dv}{dy} = \frac{1}{2}\, c_d\, \frac{\rho_0 h_0 S_e}{M_e}\, \frac{\rho v s}{\sin\gamma}\,, \qquad \frac{dm}{dy} = \frac{1}{2}\, c_h\, \frac{\rho_0 h_0 S_e}{M_e}\, \frac{V_e^2}{H^*}\, \frac{\rho v^2 s}{\sin\gamma}\,. \tag{5}$$

To find the analytical solution of Eqs. (5), we suggest that the atmosphere is isothermal: $\rho = e^{-y}$. According to B. Yu. Levin [2] we also assume that the middle section and the mass of the body are connected by the following relation

$$s = m^\mu,\ \mu = \text{const}.$$

The parameter μ characterizes the possible role of rotation during the flight.

Then the solution of Eqs. (5) with the initial conditions $y = \infty$, $v = 1$, $m = 1$ has the form

$$m = \exp\left(-\frac{\beta}{1-\mu}\left(1 - v^2\right)\right), \tag{6}$$

$$y = \ln\alpha + \beta - \ln\frac{\triangle}{2}$$

where

$$\triangle = \bar{E}i(\beta) - \bar{E}i(\beta v^2)\,,\ \bar{E}i(x) = \int\limits_{-\infty}^{x} \frac{e^z dz}{z}\,,$$

$$\alpha = \frac{1}{2}\, c_d\, \frac{\rho_0 h_0 S_e}{M_e \sin\gamma}\,, \qquad \beta = (1-\mu)\,\frac{c_h V_e^2}{2 c_d H^*}\,, \tag{7}$$

where α is the ballistic coefficient and β is the mass loss parameter.

Hereafter we will use the analytical solution (6) as the general theoretic height–velocity relation.

The Method of Calculations

The values of the parameters α and β providing for the best fit of the observed physical process can be found by the method proposed by Gritsevich [3]. The sum of the squared deviations of the actually observed altitudes h_i and velocities V_i of motion at certain points $i = 1, 2, \ldots, n$ of the desired curve described by Eq. (6) from the corresponding values e^{-y}

calculated using Eq. (6) is used as the fitting criterion. Then the desired parameters are uniquely determined by the following formulas:

$$\alpha = \frac{\sum\limits_{i=1}^{n} e^{-\beta-y_i} \cdot \triangle_i}{2\sum\limits_{i=1}^{n} e^{-2y_i}} \tag{8}$$

$$\sum_{i=1}^{n}\left[\left(\triangle_i \sum_{i=1}^{n}\exp(-2y_i) - \left(\sum_{i=1}^{n}\triangle_i \exp(-y_i)\right)\exp(-y_i)\right)\cdot\left(\triangle_i - (\triangle_i)'_\beta\right)\right] = 0 \tag{9}$$

$$\frac{\sum\limits_{i=1}^{n} e^{-2y_i}\sum\limits_{i=1}^{n}\left(\left((\triangle_i)'_\beta - \triangle_i\right)^2 + \left(\triangle_i - 2\alpha\exp(\beta - y_i)\right)\right)\left((\triangle_i)''_\beta - 2(\triangle_i)'_\beta + \triangle_i\right)}{\left(\sum\limits_{i=1}^{n}\exp(-y_i)(\triangle_i - (\triangle_i)'_\beta\right)^2} > 1 \tag{10}$$

Here

$$v_i = \frac{V_i}{V_e}\,,\; y_i = \frac{h_i}{h_0}\,,\; \triangle_i = \bar{E}i(\beta) - \bar{E}i(\beta v_i^2),\; (\triangle_i)'_\beta = \frac{d\triangle_i}{d\beta}\,,\; (\triangle_i)''_\beta = \frac{d^2\triangle_i}{d\beta^2}\,.$$

It is essentially important to note that the value of β specified by Eqs. (8)-(10) describes the mass-loss efficiency along the entire studied segment of the meteor trajectory due to both evaporation and melting of the outer layer followed by blowing-off of the liquid film by the flow and detachment of secondary-size fragments from the parent body [4]. Let's also recall here the definition of the ablation coefficient σ of a meteor body:

$$\sigma = \frac{c_h}{c_d H^*}\,. \tag{11}$$

Comparing of the expressions (11) and (7) one can see that value of the mass loss parameter β allows calculating the ablation coefficient σ according to the formula:

$$\sigma = \frac{2\beta}{(1-\mu)V_e^2}\,.$$

Influence of the parameters α and β on the impact consequences

Four main impact types can be distinguished based on the values of the parameters α and β.

1. The range $\alpha \ll 1$, $\beta \ll 1$: the impact of a unified massive body with the Earth's surface results in the formation of a vast crater. The large body's mass minimizes or entirely excludes the effect of the atmosphere. Almost certainly, the atmosphere is penetrated by a cosmic body without its fracture. An illustrative example is the Barringer crater in the state of Arizona, United States.

2. The range $\alpha < 1$, $\beta < 1$: fracture of the meteor body in the atmosphere and deposition of a fragments cloud onto the Earth's surface take place with the formation of a

crater strew field with corresponding meteorite fragments. Modern mathematical models describing the motion of the fragments cloud in the atmosphere allow us to predict basic geographic and other features of these fields. The ablation effect on the motion of the fragments is of minor importance. An illustrative example is the Sikhote–Alin meteorite shower (1947, Russia).

3. The range $\alpha \sim 1$, $\beta \sim 1$. These conditions are close to those of the preceding section. However, they are characterized by a more significant role of ablation. As obvious examples, we can indicate reliably documented fireballs for which luminous segment of atmospheric trajectory were observed, meteorite fragments being also found in a number of cases. Among them, there are famous bolides Neuschwanstein (2002, Germany), Innisfree (1977, Canada) and Lost City (1970, United States). They are relatively small meteoroids, thus the total mass of meteorites collected on the Earth's surface is in the order of 10 kg (see e.g. [8]). The absence of craters is explained by the same reason. The characteristic feature of the collected meteorite fragments is the presence of ablation traces on their outside surface covered by fusion crust.

4. The range $\alpha < 1$, $\beta \gg 1$: fracture and complete evaporation of a meteoroid in the atmosphere take place at the low velocity loss. The characteristic consequence of these events is the fall of a high-speed air-vapour jet onto the Earth's surface. Descending in the atmosphere, the gas volume expands [5]. Then, the gas cloud arrives at the Earth's surface, which is accompanied by the formation of a high-pressure region, and flows around its relief. As a result, the characteristic size of the impact region exceeds the characteristic size of the original meteoroid by several orders of magnitude. The Tunguska Event (1908, Russia) serves as a real example of an event of this type.

Results and Conclusions

In Fig. 1 the distribution of the ballistic coefficient and the mass loss parameter for the analyzed fireballs is shown: detected by European Fireball Network (based on data published by Ceplecha et al. [9]-[10]), by the Meteorite Observation and Recovery Project in Canada (based on data published by Halliday et al. [11]), and by Prairie Network (published by McCrosky et al. [12]-[13]. Additional events shown in this figure are: Crater Barringer, Tunguska, Sikhote–Alin, bolide/meteorite Neuschwanstein (European Fireball Network, 2002, Germany), bolide/meteorite Benešov (European Fireball Network, 1991, Czech Republic), bolide/meteorite Innisfree (Meteorite Observation and Recovery Project, 1977, Canada), and bolide/meteorite Lost City (Prairie Meteorite Network, 1970, United States). The curve shows the analytically derived margin between the region with expected meteorite survivors on the ground and fully ablated meteors [14]-[15]. It depends on the trajectory slope and can be derived more carefully for any individual case.

The exact values of the received parameters as well as estimating initial masses and ablation coefficient values have been published in the papers [6]-[7]. It is remarkable that in Fig. 1, the meteorite Innisfree appeared exactly at the left. It means that the ballistic coefficient for Innisfree was the smallest among all fireballs registered by the Canadian network (according to the Eq. (7), it corresponds to a quite big value of the product of initial mass and a sine of a slope). On the other hand, among all these fireballs Innisfree was the unique fall for which fragments of a meteorite have been found on the Earth surface [8].

The approximation of the actual data using theoretical models in general makes it possible to achieve additional estimates, which do not directly follow from the observations. As an example, the correct mathematical modeling of meteor events in the atmosphere is necessary for further estimates of the key parameters, including the extra-atmospheric mass, the ablation coefficient, and the effective enthalpy of evaporation of entering bodies. In turn, this information is needed by some applications, namely, those aimed at studying the problems of asteroid and comet security, to develop measures of planetary defense, and to determine the bodies that can reach the Earth surface. Surely, the detailed review of the existing models for evaluating parameters of meteor bodies deserves a separate future publication.

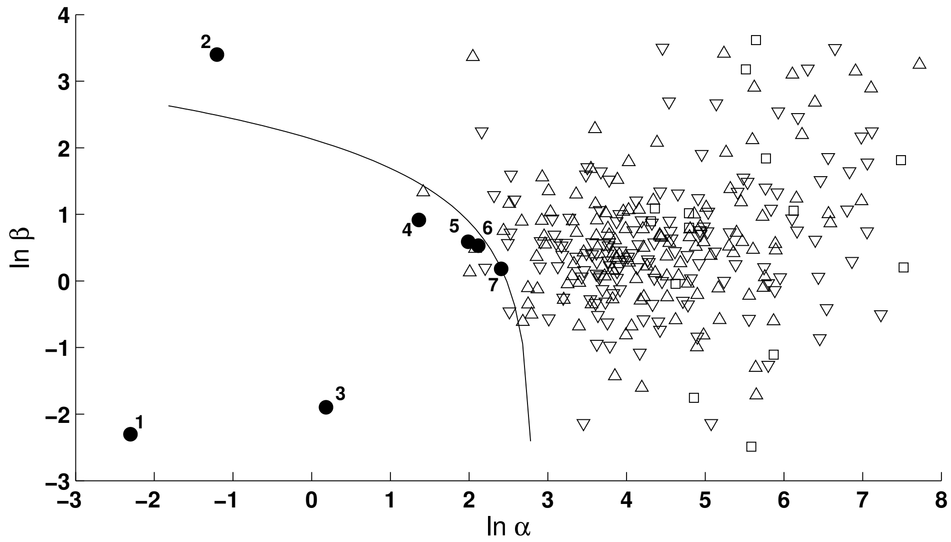

Figure 1: The distribution of the ballistic coefficient and the mass loss parameter: for the analyzed fireballs detected by European Fireball Network [9]-[10], ∇; by the Meteorite Observation and Recovery Project in Canada [11], △; by the Prairie network [12]-[13], □. Additional events, •: (1) — Crater Barringer; (2) — Tunguska; (3) — Sikhote–Alin; (4) — bolide/meteorite Neuschwanstein; (5) — bolide/meteorite Benešov; (6) — bolide/meteorite Innisfree; (7) — bolide/meteorite Lost City. The curve shows the analytically derived margin between the region with expected meteorite survivors on the ground and fully ablated meteors

References

[1] Stulov V.P., Mirskii V.N., Vislyi A.I. Aerodinamika bolidov (Aerodynamics of Bolides). Nauka, Moscow, 1995. [in Russian].

[2] Levin, B.Yu. Physical Theory of Meteors and Meteoroid Substance in the Solar System. AN SSSR, Moscow, 1956. [in Russian].

[3] Gritsevich, M.I. Approximation of the Observed Motion of Bolides by the Analytical Solution of the Equations of Meteor Physics, Solar System Research, 2007, Vol. 41, No. 6, p. 509–514.

[4] Gritsevich, M.I. Estimating the Mass of a Fireball Projectile, Doklady Physics, 2008, Vol. 53, No. 11, p. 588–593.

[5] Turchak, L.I. Braking of bodies upon entry into an atmosphere, Cosmic Research, 1980, Vol. 17, No. 6, p. 778–782.

[6] Gritsevich, M.I. Determination of Parameters of Meteor Bodies based on flight Observational Data, Advances in Space Research, 2009, Vol. 44, No. 3, p. 323–334.

[7] Lukashenko, V.T. Calculating the mass of meteoroids based on observations by the European Fireball Network, 2013, Proceedings of the Conference–Competition of Young Scientists, Institute of Mechanics. Moscow State Univ. [in Russian].

[8] Gritsevich, M.I. The Příbram, Lost City, Innisfree, and Neuschwanstein falls: An analysis of the atmospheric trajectories, Solar System Research, 2008, Vol. 42, No. 5, p. 372–390.

[9] Ceplecha, Z., Novakova–Jezkova, M., Porubcan, V., Kirsten, T., Kiko, J., and Bocek, J. European Network fireballs photographed in 1977, Bull. Astron. Inst. Czechosl., 1983, Vol. 34, p. 195–212.

[10] Ceplecha, Z., Spurny, P., Bocek, J., Novakova, M., and Polnitzky, G. European Network fireballs photographed in 1978, Bull. Astron. Inst. Czechosl., 1987, Vol. 38, p. 211–222.

[11] Halliday, I., Griffin, A.A. and Blackwell, A.T. Detailed Data for 259 Fireballs from Canadian Camera Network and Inferences Concerning the Influx of Large Meteoroids, 1996, Meteoritics & Planetary Science, Vol. 31, p. 185–217.

[12] McCrosky, R.E., Shao, C.-Y., Posen, A. Prairie Network Fireball Data I: Summary and Orbits. Preprint No. 665, Center for Astrophysics, Cambridge, Massachusetts, 1976.

[13] McCrosky, R.E., Shao, C.-Y., Posen, A. Prairie Network Fireball Data II: Trajectories and Light Curves. Preprint No. 721, Center for Astrophysics, Cambridge, Massachusetts, 1977.

[14] Gritsevich, M.I., Stulov, V.P., and Turchak, L.I. Consequences for Collisions of Natural Cosmic Bodies with the Earth Atmosphere and Surface, 2012, Cosmic Research, Vol. 50, No. 1, p. 56–64.

[15] Gritsevich, M., Kuznetsova, D., Stulov, V., and Turchak, L. Deceleration Rate of a Fireball as a Tool to Predict Consequences of the Impact, 2013, Proceedings of the International Meteor Conference 2012.

Vladimir Vinnikov, Maria Gritsevich, Dorodnitsyn Computing Center, Russian Academy of Science, Vavilova st., 40, 119991, Moscow, Moscow, Russia
Maria Gritsevich, Daria Kuznetsova, Vladislav Lukashenko, Institute of Mechanics, Lomonosov Moscow State University, Michurinsky Ave., 1, 119192, Moscow, Russia
Maria Gritsevich, Daria Kuznetsova, Vladislav Lukashenko, Faculty of Mechanics and Mathematics, Lomonosov Moscow State University, Leninskiye Gory, 1, 119991, Moscow, Russia